"Semiconductor" model of the "polymer-CNTs" composite strengthening

Liudmyla A. Karachevtseva[1], Mykola T. Kartel[2], Oleg O. Lytvynenko[1], Volodymyr F. Onyshchenko[1]

[1] V. Lashkaryov Institute of Semiconductor Physics, NASU, Prsp. Nauki, 41, Kiev-03028, Ukraine.
[2] O. Chuiko Institute of Surface Chemistry, NASU, 17 General Naymov Street, Kyiv 03164 Ukraine.
lytvole@gmail.com

1. Subject of study

Multiwall carbon nanotubes (CNTs) are among the most anisotropic materials known and have extremely high values of Young's modulus. Carbon nanotube aspect ratio of length to diameter is more than 10^3; this distinguishes it from other nanoparticles.

We investigated the opportunities to enhance the properties of nanostructured surfaces "polymer-multiwall carbon nanotube" composites at 300 K. It was confirmed connection between the composite IR absorption at in the spectral area of sp^3 hybridization bonds and the primary amino group, $\gamma_{as}(CH)$ and $\gamma_{as}(CH_2)$ vibrations. We measured IR reflectance maxima in the spectral area of CH valence and deformation vibrations after formation of composite "rubber-carbon nanotube". The IR peak dependencies on the CNT content at spectral area of sp^3 hybridization bonds are described by a 1D Gaussian curve for the diffusion equation in the electric field between electrons of nanotubes and protons in polymer. It determines the "semiconductor" n-p model to improve the strength properties of composite films of polyethylenimine, polyamide and polypropylene with multiwall (CNTs) due to the composite structuring supported by vibrations in the intrinsic electric field.

2. Experimental

Carbon high purity multiwall (CNTs) of 2 μm length and 20 nm diameter (Fig. 1) were obtained by catalytic pyrolysis of unsaturated hydrocarbons.

Nanoparticle morphology was investigated by X-ray microscopy (JSM-35-C). The composites were made of polyethylenimine, polypropylene and polyamide filled by a mixture of CNTs with the polymer powder and dried; composite samples were formed by hot pressing. Compression and tension tests of the polymeric materials and their composites were measured by tensile machine 2167-R50 with automatic recording of the deformation diagram. Thin polymeric films (100-150 μm thick) without and with CNTs were prepared out using Thermo HYDROPRESS. Chemical states in composites were identified by IR absorption and reflectance spectra using a PerkinElmer Spectrum BXII IR Fourier spectrometer in the spectral range of 300-8000 cm^{-1}. The optical absorption spectra were measured at normal incidence of IR radiation on the
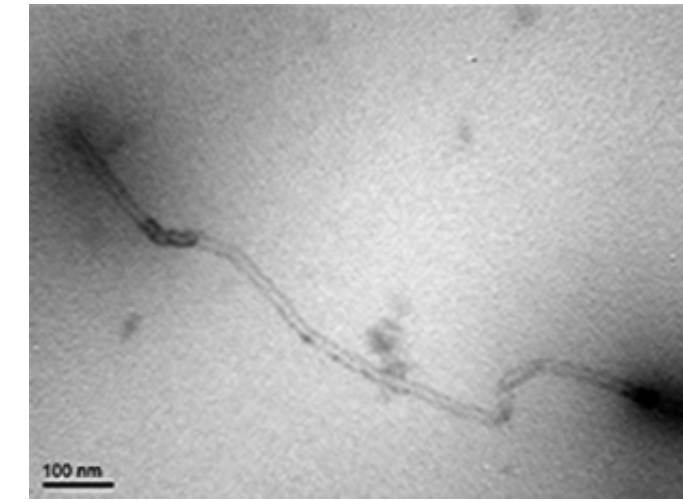

Fig. 1. Morphology of carbon multiwall nanotube according to X-ray microscopy.

3. Results and Discussion

Fig. 2a shows IR spectra of polyethylenimine (curve 1), the composite "polyethylenimine-carbon nanotubes" (curve 2) and the ratio of spectra 1 and 2 (curve 3). Fig. 2b shows IR absorption by N-H(1) (curve 1) and N-H(2) (curve 2) bonds in composites based on polyethylenimine (PEI) vs the carbon nanotube content in polymer.

After formation of the "polyethylenimine-carbon nanotubes" composite intensive absorption maxima were measured in area of the sp^3 hybridization (D) bonds at the frequency of N-H(1) oscillations in the primary amino group of PEIs and in area of the sp^2 hybridization (G) bonds for the N-H(2) oscillation frequencies in secondary amino group of PEIs (Fig. 2a and 2b).

Fig. 3a shows IR absorption spectra of polyamide (curve 1), "polyamide-carbon nanotubes" composite (curve 2) and the ratio of the curves 1 and 2 (curve 3).

After adding CNTs to polymers (concentration of 0.25%), IR absorption of "composite/polymer" films exceeds that of polymer films essentially. Higher C-C fluctuations, CH, CH_2 and CH_3 bond absorption correspond to higher IR absorption of composites at the frequencies of sp^3 hybridization bonds (Fig. 3b).

From Fig. 4a one can see that after adding CNTs (concentration of 0.25%) to polypropylene IR absorption exceeds the absorption of polypropylene 4-8 times in all measured spectral range. This increases the intensity of the C-C bond vibrations (835 and 1000 cm^{-1}, $\gamma_r(CH_3)$ (A) - 970 cm^{-1}, $\gamma_{as}(CH_3)$ - 1170 cm^{-1}, $\gamma_{as}(CH)$ (A) on the frequency of bonds sp^3 hybridization (D) - 1360 cm^{-1}, as well as fluctuations $\delta(CH_3) - 1380$ cm^{-1}, $\delta(CH_3) - 1440$ cm^{-1}, $\delta_s(CH_3) - 1470$ cm^{-1}.

After formation of the "polypropylene-carbon nanotubes" composite intensive absorption maxima were measured in area of the sp^3 hybridization (D) bonds at the frequency of $\gamma_{as}(CH)$ vibrations (Fig. 4b). Higher C-C fluctuations, CH, CH_2 and CH_3 bond absorption correspond to higher absorption of composites at the frequencies of sp^3 hybridization bonds.

IR reflectance maxima of composite "rubber-carbon nanotube" are measured at 2.5% CNTs (Fig. 5a) in the area of CH deformation vibrations at frequencies 1297 cm^{-1}, 1466 cm^{-1} and 1728 cm^{-1} and valence vibrations at frequencies 2844 cm^{-1} and 2914 cm^{-1}.

Fig. 5b shows dependences of relative IR reflectance R/R_0 of composite "polybutadien rubber-carbon nanotube" on the carbon nanotube content in the area of CH_3 (curve 1, 2844 cm^{-1}) and CH_2 (curve 2, 2914 cm^{-1}) valence vibrations and relative tensile strength N/N_0 for two types of composites (curves 3-4).

There are maxima of dependences 1-4 from Fig. 5b at 0.16, 1.25 and 2.5 wt% CNTs and pronounced minimum at 5 wt% CNTs. That minimum corresponds to minima IR reflectance of CH_3 and CH_2 valence vibrations. In addition, at high CNTs content (> 5 wt% CNTs) dependences 3 and 4 from Fig. 5b became almost linear and proportional to CNTs surface in composite.

IR absorption in spectral area of sp^3 hybridization bonds in composites of polymers with multiwall carbon nanotubes has maxima (Figs 2b, 3b, 4b and 5) at its dependencies on CNT content. Thus, the maxima correspond to fixed distance between nanotubes. According to 2D model of CNTs distribution distance between nanotubes in composites depends on the CNTs concentration (N_{CNT}), its content (wt% CNT) and the nanotube volume (V_{CNT}):

$$a = (N_{CNT})^{-1/2} = (\% \, CNT/100 V_{CNT})^{-1/2} \quad (1)$$

Fig. 2: a - IR spectra of polyethylenimine (curve 1), the composite "polyethylenimine-carbon nanotubes" (curve 2) and the ratio of spectra 1 and 2 (curve 3); b - IR absorption by N-H(1) (curve 1) and N-H(2) (curve 2) bonds in composites based on polyethylenimine vs the carbon nanotube content in polymer.

Fig. 3: a - IR absorption spectra of polyamide (curve 1), "polyamide - carbon nanotubes" composite (curve 2) and the ratio of the curves 1 and 2 (curve 3); b - IR absorption at the frequencies of sp^3 hybridization bonds (D) in composites based on polyamide-6 vs the carbon nanotube content in polymer.

The IR absorption maximum in area of sp^3 hybridization bonds (D) of composite polyethylenimine-carbon nanotubes (Fig. 2b) corresponds to the average distance $a = 0.31$ μm between the cylindrical CNT (diameter of 20 nm, length of 2 μm). The IR absorption maximum for sp^3 hybridization bonds (D) of composites polyamide-carbon nanotubes and polypropylene-carbon nanotubes (Fig. 3b and Fig. 4b) corresponds to the average distance $a = 0.35$ μm between the cylindrical CNTs.

Obtained maxima one can explained by the geometric factor - characteristic volume around the cylindrical CNT at a distance of $a_m/2$ from nanotubes. As $a > a_m$, the characteristic volume around CNT increases due to increasing of the content of CNT - % CNT, N_{CNT}, IR absorption increases too. The characteristic volume around CNT and IR absorption decreases with growth of CNT content at $a < a_m$. Surface of all nanotubes in composites S_{CNT} is proportional to the concentration of CNT (N_{CNT}) and have not peak in dependence on CNT content as in Figs 2b, 3b, 4b and 5.

Fig. 6 shows the calculated (according to Equation (1)) dependences of average distance a between CNT (curve 1), geometric approximation (curve 2, characteristic volume around CNT), experimental dependence from Fig. 4b of the IR absorption peak in area of sp^3 hybridization of "polypropylene-CNTs" composite on CNT content. The obtained geometric approximation (Fig. 6, curve 2) explains qualitatively only the experimental dependence of IR absorption peak in bonds sp^3 hybridization (D) of "polypropylene-carbon nanotube" composite on the CNT content. This relationship is more nonlinear and has the form of a 1D Gaussian curve (Fig. 6, curve 3), which corresponds to the diffusion equation in the electric field.

The intrinsic electric field between electrons of nanotubes and protons in polymer matrix is determined by band bending and has a space charge region (SCR) of width w (Fig. 7).

$$\frac{1}{r}\frac{\partial}{\partial r}\left(r\frac{\partial Y}{\partial r}\right) = -\frac{\rho_q}{\varepsilon \varepsilon_0}\frac{e}{kT} \quad (2)$$
where: r - the radius vector, ρ_q - the charge density.

We used next the boundary conditions for the area of the SCR width w for a cylindrical nanotube with diameter d: $E(d/2 + w) = 0$, $Y(d/2 + w) = 0$, $Y(d/2) = Y_S$, where E is the electric field strength, Y_S - the value of the potential on the surface of the nanotube.

Integrating Eq. (2) and using the above boundary conditions, we obtained next equation:

$$\frac{16\varepsilon\varepsilon_0 Y_S w}{eq_v d^2} - 1 + \left(1 + \frac{2w}{d}\right)^2\left(1 - 2\ln\left(1 + \frac{2w}{d}\right)\right) = 0 \quad (3)$$

Fig. 8 shows dependences of the size of the space charge region of cylindrical nanotubes calculated from Eq. (3) on their diameter at various values of the surface potential.
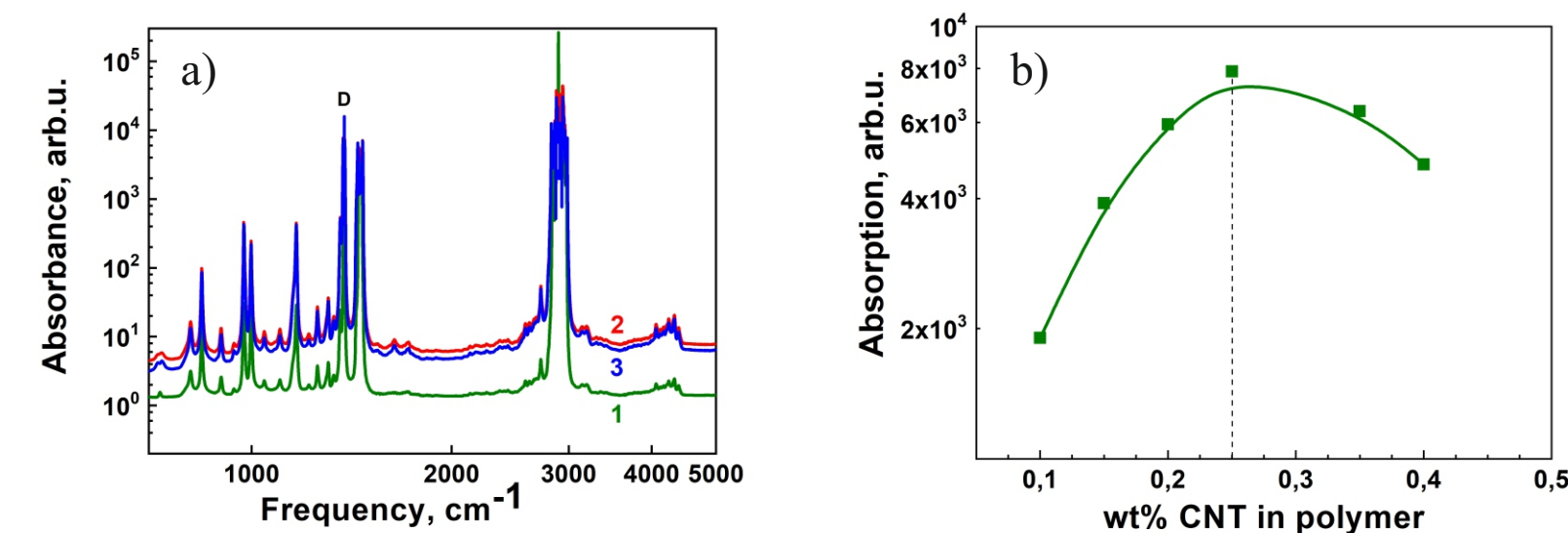

Fig. 4: a - IR absorption spectra of polypropelene (curve 1), composite "polypropylene-carbon nanotubes" (curve 2) and the ratio of curves 1 and 2 (curve 3); b - IR absorption by sp^3 hybridization bonds (D) in composites based on polypropylene vs the carbon nanotube content in polymer.
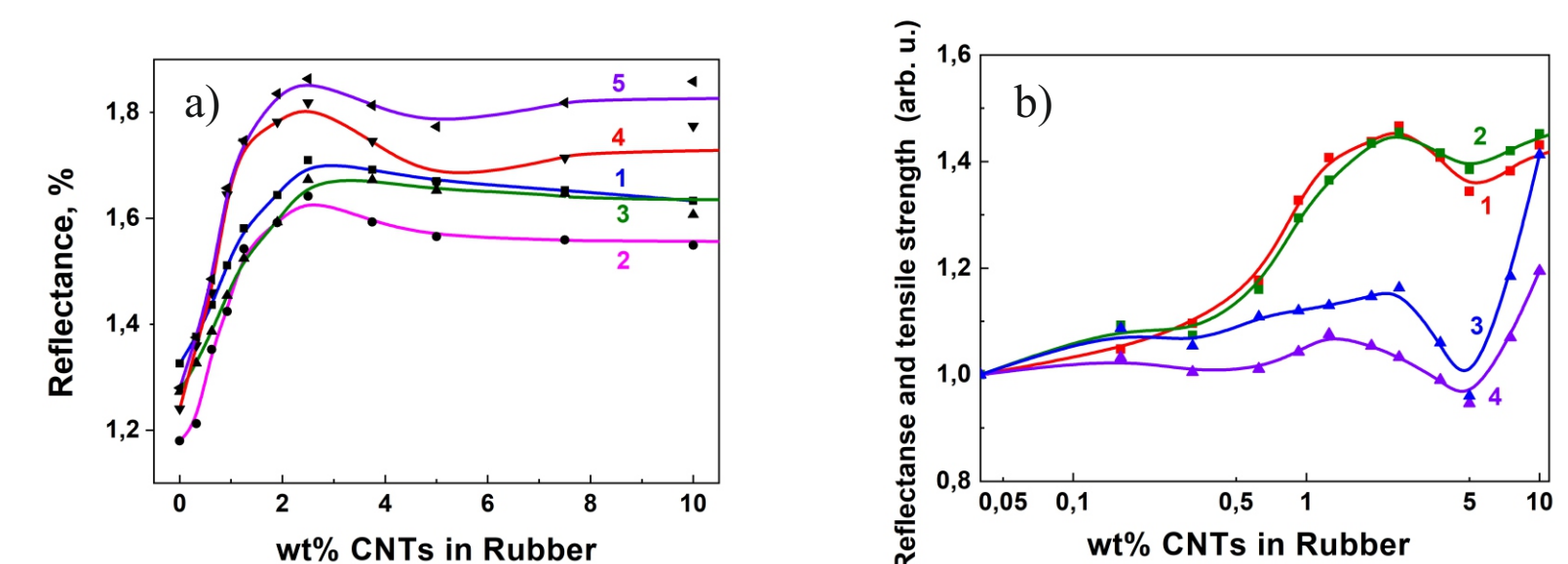

Fig. 5: a - IR reflectance maxima of composite "rubber-carbon nanotube" vs the carbon nanotube content in polymer in the area of CH deformation vibrations (1, 2 and 3) and valence vibrations (4, CH_3 and 5, CH_2); b - Relative IR reflectance R/R_0 in the area of CH_3 (curve 1) and CH_2 (curve 2) valence vibrations and the relative tensile strength N/N_0 for two types of composites "polybutadien rubber-carbon nanotube" (curves 3-4) vs the carbon nanotube content in rubber.
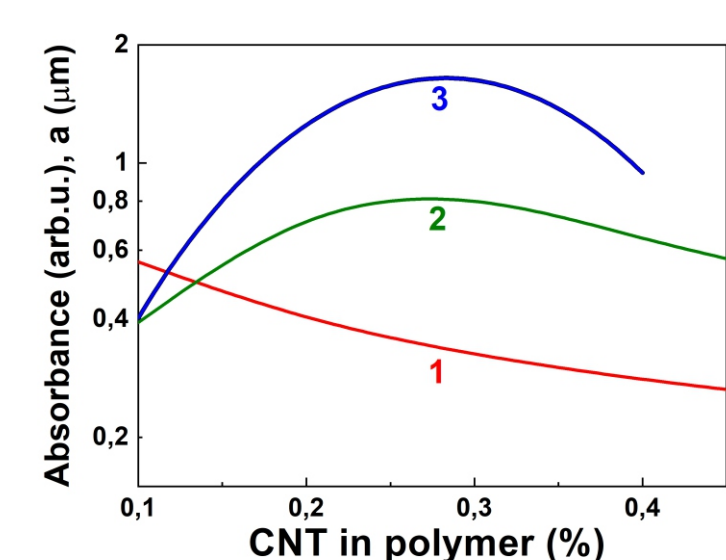

Fig. 6. Dependences on CNTs content of: (1) average distance a between CNT, (2) geometric approximation – characteristic volume around CNT; (3) experimental dependence from Fig. 4b.

Fig. 7. Band bending and SCR width w at the "polymer-CNTs" boundary.

Fig. 8 shows that the SCR width w decreases with the diameter of nanotubes decrease. The length a = 310 nm between cylindrical CNT corresponds to the distance between nanotubes $w = (a_m - d)/2 = 155$ nm in composite "polyethylenimine-carbon nanotubes" for maximum of IR absorption (Fig. 2b) and surface potential $Y_S = -3kT$ (79.5 mV) and electric field intensity $E = Y_S/w = 5.12 \cdot 10^3$ V/cm. The length a = 35 nm between cylindrical CNT corresponds to the distance between nanotubes $w = (a_m - d)/2 = 170$ nm in composites "polyamide-carbon nanotubes" and "polypropylene-carbon nanotubes" (Fig. 3b and Fig. 4b) for maximum of IR absorption. It corresponds to surface potential $Y_S = -4kT$ (106 mV) (Fig. 8), electric field intensity $E = Y_S/w = 6.3 \cdot 10^3$ V/cm for $w = 170$ nm between cylindrical CNTs (diameter of 20 nm, length of 2 μm) at maximum at IR absorption peak in area of bonds of sp^3 hybridization (D).

Carbon nanotubes divided into two main groups: (1) the molecular associated nanotubes linked through weak short-acting interactions, van der Waals forces, (2) nanotubes with additional strong covalent sp^3 type C-C bonding for long-acting interactions.

The recent advances in both the production and characterization of composites "polymer-CNTs" for first case enabled the expansion of composite reinforcement levels to the nanometer scales of short-acting interactions. Molecular dynamics simulations demonstrate the formation of an ordered layer of polymer matrix surrounding the nanotube. This thin layer, known as the interphase, not determines at low (0.1-0.5) % CNTs concentration the overall mechanical response of the composite as the only reinforcement phase. But at high CNTs content (> 5 % CNTs) dependences for tensile strength became almost linear and proportional to CNTs surface in composite.

For second case, the way to improve the strength properties of composites "polymer-CNTs" is the polymer crystallization. For the long-acting hundreds nanometer interactions, the polymer crystallization depends on sp^3 C-C bonds organization in the intrinsic electric field and according to "semiconductor" n-p model. As a result, the profile analysis of X-ray reflexes confirmed high crystallinity degree of investigated "polymer-CNTs" composites - from 72% to 85%. Crystalline polymers demonstrate high tensile strength (30-40 MPa for composite "polyamide 6–CNTs").
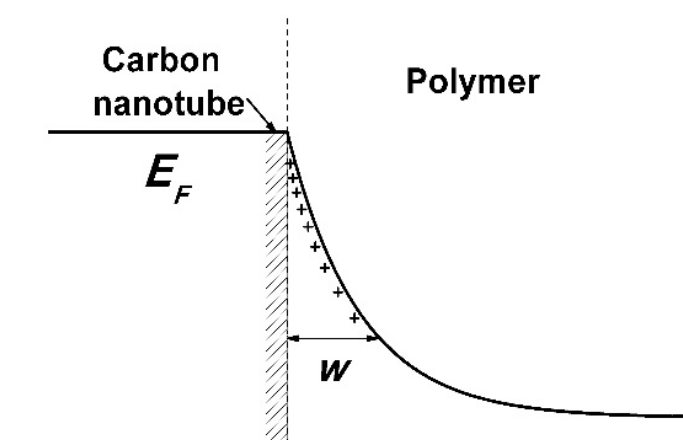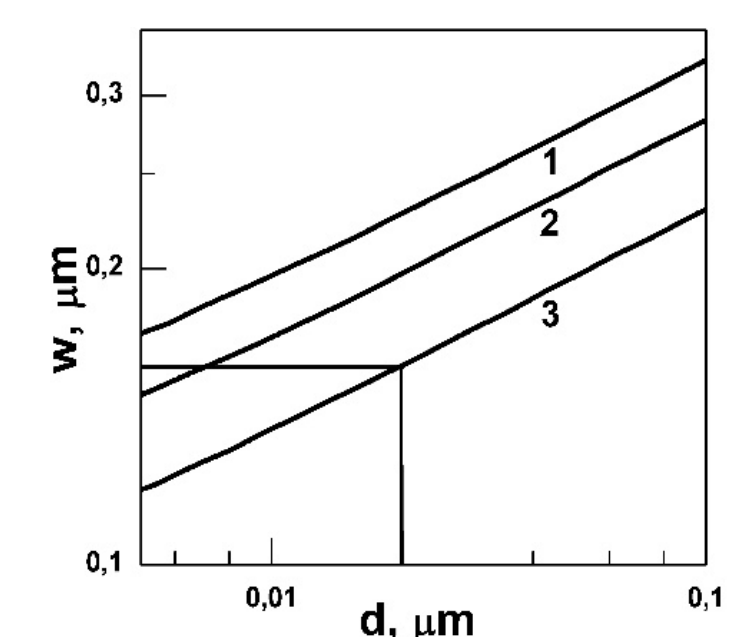

Fig. 8. Dependence of SCR width w around cylindrical nanotubes on its diameter for surface potential Y_S: 1-12 kT; 2 - 8 kT; 3 - 4 kT.